Available online at www.sciencedirect.com

ScienceDirect

Energy Procedia 55 (2014) 356 – 360

Energy Procedia

4th International Conference on Silicon Photovoltaics, SiliconPV 2014

# Laser-welded interconnection of screen-printed Si solar cells

Henning Schulte-Huxel[a,*], Susanne Blankemeyer[a], Verena Steckenreiter[a], Sarah Kajari-Schroeder[a], Rolf Brendel[a,b]

[a]*Institute for Solar Energy Research Hamelin (ISFH), Am Ohrberg 1, D-31860 Emmerthal, Germany*
[b]*Institut für Festkörperphysik, Leibniz Universität Hannover, Appelstraße 2, D-30167 Hannover, Germany*

**Abstract**

We demonstrate the laser welding of Al interconnects to the BSF rear-side of screen-printed two-side-contacted solar cells. The Al paste on the rear side of solar cell is laser-welded to an Al foil. This reduces the silver consumption of the solar cells by making silver pads on the rear side obsolete. Our proof-of-concept modules are free of laser damage. A 3-cell-module from 6” solar cells shows no change in fill factor within the statistical measurement uncertainty after artificial aging in 500 humidity-freeze cycles.


Peer-review under responsibility of the scientific committee of the SiliconPV 2014 conference

*Keywords:* Laser micro welding; module integration; cell interconnection; Al metallization; Al paste; Screen printed solar cells; PERC solar cells

## 1. Introduction

Material cost reduction and efficiency increase are key factors for cost reduction in photovoltaics. Apart from the wafer itself the metallization, especially Ag, are the most expensive materials in the current cell technology [1]. Omitting the silver pads on the rear side reduces the total Ag consumption by one fourth [2] and improves the efficiency by reduction of recombination. An increased recombination occurs underneath the Ag pads since there no aluminum back surface field (BSF) can be formed [3]. Avoiding Ag pads has shown an efficiency advantage of 0.1 to 0.4% absolute [4].

Although screen-printed Al for rear side metallization has been used since decades [5], a direct contacting of the

* Corresponding author. Tel.: +49-5151-999-303; fax: +49-5151-999-400.
*E-mail address:* h.schulte-huxel@isfh.de

1876-6102 
Peer-review under responsibility of the scientific committee of the SiliconPV 2014 conference
doi:10.1016/j.egypro.2014.08.102

Al paste is still a challenge, since Al forms a highly stable oxide on its surface. Solderable contacts without Ag pads were demonstrated by applying tin [4] or tin alloys [6] using ultra-sonic soldering to the Al paste.

Here we pursue a different route to omit the silver pads on the rear side of screen-printed solar cells: We integrate the solar cells into a module by laser welding the sintered Al paste of BSF solar cells to an Al foil.

## 2. Laser welding of the rear contact

We start with three screen-printed solar cells with a full area aluminum BSF fabricated on *p*-type Czochralski grown Si-wafer (156 mm × 156 mm). The solar cells are in-house-fabricated and have no Ag pads on the rear side. For contacting the back side we use a 10-µm-thick household Al foil, which is thermally attached to an encapsulant of 450 µm in thickness (Tectosil®, Wacker). This encapsulant substrate is in the size of the final module. Additionally, in this step grooves are embossed where the ribbons for interconnection will be located. We structure the Al foil such that the base contacts of the individual cells are isolated from each other. To the front side of solar cells we solder standard Cu ribbons, which are coated with solder and are 2 mm wide. Then the solar cells are placed on the substrate with the Al foil and the ribbons of one cell are led to the rear side of the next cell between the Al-foil and the rear side metallization of the cell. We apply the aluminum-based mechanical and electrical laser interconnection (AMELI) process [7]. A pulsed laser beam of 1.3 µs pulse duration is focused through the encapsulant into the Al foil, see Fig. 1. We use laser pulses emitted at 1064nm and with an energy of 2 mJ. The Al foil melts and fuses with the sintered Al paste. In the same process the Al foil is also welded to the Cu ribbons. Therefore, the ribbons, which are soldered to the front side of one cell, are contacted to the rear side of the next solar cell. By this a series interconnection is enabled. For final encapsulation we laminate the module in a glass-glass configuration. The lamination foil used a substrate carrying the Al foil fulfills in the final lay-up its function as encapsulant.

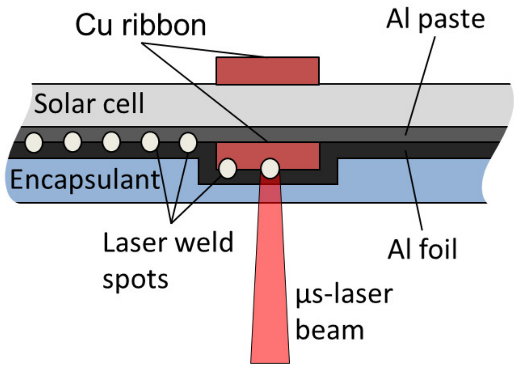


Fig. 1. Schematic of the laser-welding process (not in scale). On the front side the Cu ribbon is soldered to the cell metallization, on the rear side it is positioned between the Al foil and the Al cell metallization. The substrate with Al foil is embossed at the location of the Cu ribbon. Then the laser welding is performed on the whole rear side of the cell, welding the Al foil to the sintered Al paste

The Al paste has to meet certain requirements for the laser welding process to be applied successfully: In general the Al paste has a porous structure consisting of sintered Al spheres. This porous structure of the paste needs to be sufficiently stable in order to withstand the laser welding process and support the mechanical contact. As shown by other groups the stability depends on the composition of the paste [6]. Furthermore, the surface of the Al paste needs to be flat and free of particles as elevations on the surface may act as a spacer between the Al paste and the Al foil. This complicates the laser welding process, in which the gap between the layers should be as small as possible. In order to fulfill these requirements one needs to take care about the choice and processing of the pastes.

### 3. Proof-of-concept modules

Figure 2 a) shows a photograph of the proof-of-concept module consisting of three 6” solar cells interconnected in series. The structure of the Al foil is shown in Fig. 2 b). The horizontal lines visible in the Al foil are the embossments for the Cu ribbons.

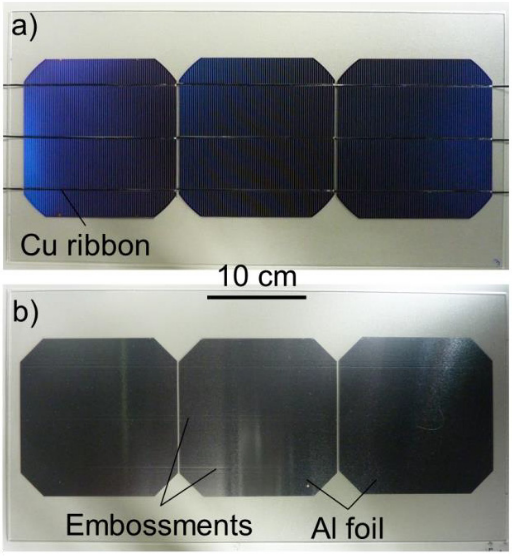


Fig. 2. Photograph of a) the proof-of-concept module consisting of three 6” solar cells and b) a part of the substrate used. Both images have the same scale.

Table 1 shows the *I-V*-characteristics of the cell before interconnection and of the module. We characterize the cells using a LOANA solar cell analysis system (pv-tools). The module before and after lamination is measured using a module flasher (h.a.l.m. Elektronik GmbH). Comparing the open circuit voltage $V_{oc}$ of the module with the sum of the $V_{oc}$ of the individual cells, we do not observe any change within the measurement uncertainty. This indicates that no laser damage was induced. The short circuit current $I_{sc}$ of the module is higher than the lowest $I_{sc}$ of the individual cells, which limits the current of the module. The fill factor FF reduces due to the resistive losses in the ribbon soldered to the front side. This is not taken into account in the cell measurements, where the current is collected at multiple points from the busbar. However, the change in FF is as low as in case of other interconnection schemes [6]. After laminating the module with a front and a rear glass, the efficiency decreases due to light reflection at the front side.

Table 1. Measured values of the individual cells before interconnection and of module II after interconnection. Additionally the calculated values in the case of a loss free interconnection is given. Measurements are related to cell are and are performed without using a shadow mask.

| Cell/ Module | $\eta$ (%) | $V_{oc}$ (mV) | FF (%) | $I_{sc}$ (mA) | $A$ (cm²) |
|---|---|---|---|---|---|
| Cell 1 | 17.2 | 618 | 79.3 | 8102 | 231 |
| Cell 2 | 18.4 | 634 | 79.3 | 8474 | 231 |
| Cell 3 | 18.4 | 632 | 79.6 | 8433 | 231 |
| Module calculated | | 1884 | | 8102 | 693 |
| Module before lamination | 17.0 | 1880.5 | 76.8 | 8112 | 693 |
| Module after lamination | 16.4 | 1870.5 | 77.1 | 7878 | 693 |

We artificially age this module with humidity-freeze cycles between -40°C and +85°C at 85% relative humidity. The in-house artificial aging test consists of 200 humidity-freeze cycles according to IEC 61215 10.12 with reduced humid time of 6 hours. This test sequence combines the required 200 thermal cycles, 1000 h damp-heat, and the humidity-freeze test. The goal is to rapidly reveal and understand failures due to chemical reactions or thermal-mechanical cycling under humid conditions.

The relative changes of the *I-V*-parameters are shown in Fig. 3. The $V_{oc}$ and FF show no degradation after 500 humidity-freeze cycles, which is the 2.5 fold of the in-house test. This proofs the long term stability of the interconnection, since an increased resistance would have reflected in a decreased fill factor. The current $I_{sc}$ decreases by less than 1 % after 200 humidity-freeze cycles and by 2.7% after 500 cycles due to the degradation of the optical properties (delamination and browning) of the encapsulant. The losses in the efficiency are well below 1.1% after 500 humidity-freeze cycles and within the uncertainty of the measurement.

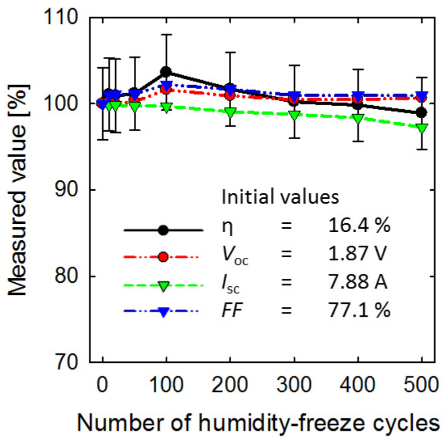


Fig. 3. Relative changes of the characteristic module *I-V*-parameters after artificial aging.

## 4. Discussion and conclusion

We have presented a process for contacting the screen-printed rear side Al-metallized of full area BSF solar cells by laser welding. We observe no detectable damage of the cells after laser welding. A proof-of-concept module with a string of 6" solar cells is stable in fill factor and open circuit voltage under 500 cycles of artificial aging and shows only 1.1% relative losses in the efficiency due to degradation of the encapsulant.

This process makes silver pads on the rear side obsolete and has thus a potential for cost reduction and efficiency increase. Costs can be decreased by reducing the silver consumption and avoiding one screen-printing step. The efficiency increase can be achieved by the reduction of the recombination due to the full coverage of the rear side by the Al BSF. Further, the laser welding of the highly conductive Al foil to the total rear side enhances the lateral current transport on the rear side. Thus, the process offers the possibility to reduce resistive losses in the rear side metallization.

The laser welding process also significantly reduces the thermo-mechanical stress due to differences in the thermal expansion coefficients of Cu and Si induced during soldering, since the heat is applied highly localized by the laser. However, in this work we soldered Cu ribbons to the front side. A direct welding of the ribbon is not possible with this laser process due to the thickness of the Cu ribbon (about 200 µm). As known from metal wrap through (MWT) solar cells single side soldering is a critical process [8,9]. Therefore, it would be favorable to contact the solar cells front side by e.g. conductive adhesives, which have shown to reduce significant the induced mechanical stress [9,10]. Alternatively, solar cells with both contacts on the rear side could be used, where the thickness of the interconnects can be reduced, since no optical shading occurs. This would enable a laser welding of both polarities [7].

Here we have shown the contacting of solar cells with full area BSF, but the process can be applied in the same way also to passivated emitter and rear cell (PERC) or other solar cells with an Al metallization. The metallization might be screen printed or also deposited by evaporation [7].

## Acknowledgements

The authors thank U. Baumann for cell processing and I. Kunze for her support. This work was supported by the German Ministry for the Environment, Nature Conservation, and Reactor Safety under Contract 0325192 (CrystalLine Project) and the State of Lower Saxony.

## References

[1] International Technology Roadmap for Photovoltaic (ITRPV) 2013 Results; 2014. Available from: itrpv.net/.cm4all/iproc.php/Reports%20downloads/ITRPV_2014_Roadmap_140314_web_z.pdf?cdp=a.
[2] Hamann L, Haas M, Wille W, Mattheis J, Zapf-Gottwick R. 30% Silver Reduction in Rear Bus Bar Metal Paste. Energy Procedia 2013;43:72–79.
[3] Kiefer F, Brendemühl T, Berger M, Lohse A, Kirstein S, Braun N, Lehr M, Heinemeyer F, Jung V, Morlier A, Blankemeyer S, Kunze I, Winter R, Harder N, Dullweber T, Köntges M, Brendel R. Influence of Solder Pads to PERC Solar Cells for Module Integration. Energy Procedia 2013;38:368–374.
[4] Campe H von, Huber S, Meyer S, Reiff S, Vietor J. Direct tin-coating of the aluminum rear contact by ultrasonic soldering. Proc. 27th EU PVSEC 2012: 1150–1153.
[5] Ralph EL. Recent advancements in low cost solar cell processing. Proc. 11th IEEE PVSC 1975:315–316.
[6] Schmitt P, Eberlein D, Ebert C, Tranitz M, Eitner U, Wirth H. Adhesion of Al-metallization in Ultra-sonic Soldering on the Al-rear Side of Solar Cells. Energy Procedia 2013;38:380–386.
[7] Schulte-Huxel H, Blankemeyer S, Bock R, Merkle A, Kajari-Schröder S, Brendel R. Al-Foil on Encapsulant for the Interconnection of Al-Metalized Silicon Solar Cells. IEEE J. Photovoltaics 2013;3(1):77–82.
[8] Eitner U, Eberlein D, Tranitz M. Interconnector-Based Module Technology for Thin MWT Cells. Proc. 27th EU PVSEC 2012:3461–3464.
[9] Bultman JH, Eikelboom DWK, Kinderman R, Tip AC, Tool CJJ, van den Nieuwenhof MACJ, Schoofs C, Schuurmans FM, Weeber AW. Fast and easy single step module assembly for back-contacted c-Si solar cells with conductive adhesives. Proc. 3rd WCPEC 2003:979–982.
[10] Bennett IJ, Jong PC de, Kloos, M. J. H., Stam, C. N. J., Henckens A., Schuermans J, Gomez RJ, Sánchez-Friera P, Lalaguna, B., Schmidt, H. Low-stress interconnection of solar cells. Pro. 22nd EU PVSEC 2007:2674–2678.